Supplementary information – Excited-state relaxation of hydrated thymine and thymidine measured by liquid-jet photoelectron spectroscopy: experiment and simulation

Franziska Buchner,[†] Akira Nakayama,[*,‡] Shohei Yamazaki,[¶] Hans-Hermann Ritze,[†] and Andrea Lübcke[*,†]

Max-Born-Institut für nichtlineare Optik und Kurzzeitspektroskopie, Max-Born-Straße 2A, 12489 Berlin, Germany., Catalysis Research Center, Hokkaido University, Sapporo 001-0021, Japan, and Department of Frontier Materials Chemistry, Graduate School of Science and Technology, Hirosaki University, Hirosaki 036-8561, Japan

E-mail: nakayama@cat.hokudai.ac.jp; luebcke@mbi-berlin.de

S1 Detection efficiency of photoelectrons at low kinetic energy

We have mentioned in the manuscript that our liquid jet spectra lack intensity at very low kinetic energies. We will first show that this is not due to the spectrometer itself. In Fig. S1

[*]To whom correspondence should be addressed

[†]Max-Born-Institut für nichtlineare Optik und Kurzzeitspektroskopie, Max-Born-Straße 2A, 12489 Berlin, Germany.

[‡]Catalysis Research Center, Hokkaido University, Sapporo 001-0021, Japan

[¶]Department of Frontier Materials Chemistry, Graduate School of Science and Technology, Hirosaki University, Hirosaki 036-8561, Japan

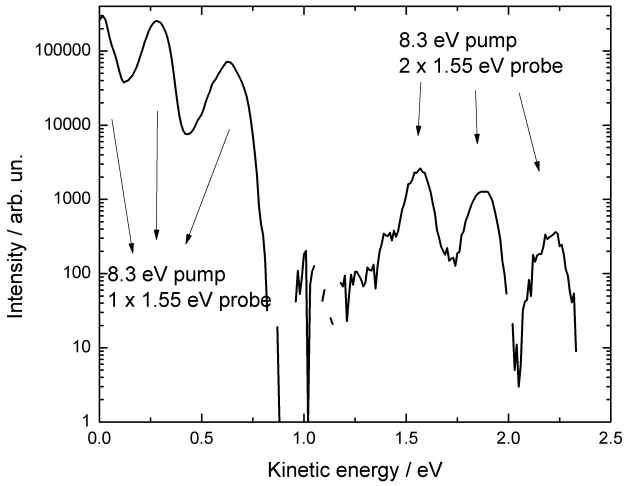

Figure S1: Gas phase spectrum of nitric oxide (NO) obtained with the same spectrometer used in the present work

we show a typical gas phase spectrum of nitric oxide (NO) obtained with the spectrometer used for the present work. Photon energies were 8.3 eV for the pump pulse and 1.55 eV for the probe pulse. The three peaks at low kinetic energies (< 1 eV) are due to a (1+1) photon 2-color photoionization process, while the second group of peaks is due to a (1+2) photon process. The final ionic states are NO^+ ($X^1\Sigma^+$, $\nu^+ = 0 - 2$) for both sets of signal[S1] and we expect the same relative intensities of the three peaks in the two groups of peaks. Deviations are therefore due to the instrument function. For the (1+1) photon process we observe an intensity ratio of the three pulses of 1.14:1:0.28 and for the (1+2) photon process 1.79:1:0.25. The peak at zero kinetic energy is mildly reduced (by some 40%). However, the intensity ratio between the second (0.28 eV and 1.87 eV) and the third peak in each group roughly retain their proportionality. Therefore, we can safely conclude that the spectrometer does not show a reduced transmission for photoelectrons at low kinetic energies > 0.3 eV, i. e. the reduced signal at low kinetic energies in liquid jet spectroscopy seems to originate from the liquid jet itself. A possible reason are charged clusters that we have previously suggested to be present around the jet.[S2]

We will now show that although there is a reduction of transmission at low kinetic energies in liquid jet experiments, the transmission around 0.5 eV is still sufficiently high to allow for detection of photoelectrons. We argue that due to the low concentration of DNA bases (1 mM) and much higher salt concentration (30 mM), the structure of these charged clusters should be the same for different DNA bases but otherwise identical solutions. Therefore, we should expect the same transmission function for those solutions and differences in the spectra are solely due to the different electronic structure of different DNA bases. In other words, a single spectrum that shows significant signal at $\sim$ 0.5 eV should be enough to proof sufficient transmission at this kinetic energy. In Fig. S2 we show one-color spectra for different DNA bases. The signal for Thd is indeed very low at around 0.5 eV, but in particular for the pyrimidine nucleosides (adenosine and guanosine) the signal is only slightly reduced compared to the peak maximum and shows that transmission is sufficiently high at this energy. Given that the expected photoelectron band from the $n\pi^*$ state is inhomogeneously broadened (peak width $\sim$ 1 eV) in solution, detection of corresponding photoelectrons should easily be possible.

S2 Electron scattering and electron range in liquid water

Static liquid jet photoelectron spectroscopy of liquids was pioneered by Winter and coworkers[S3] exploiting extreme ultraviolet (euv) pulses. Those spectra exhibit strong contributions from inelastically scattered photoelectrons at lower energies than originally generated. However, in the present work, photoelectrons at low kinetic energies are generated and inelastic scattering is not important. The inelastic scattering cross-sections depend on the kinetic energy of the photoelectrons. Plante et al. have calculated the cross-sections for different processes in liquid water for electron kinetic energies in the range between 1 eV and 100 MeV.[S4] Ionization and electronic excitations are important only for electron kinetic

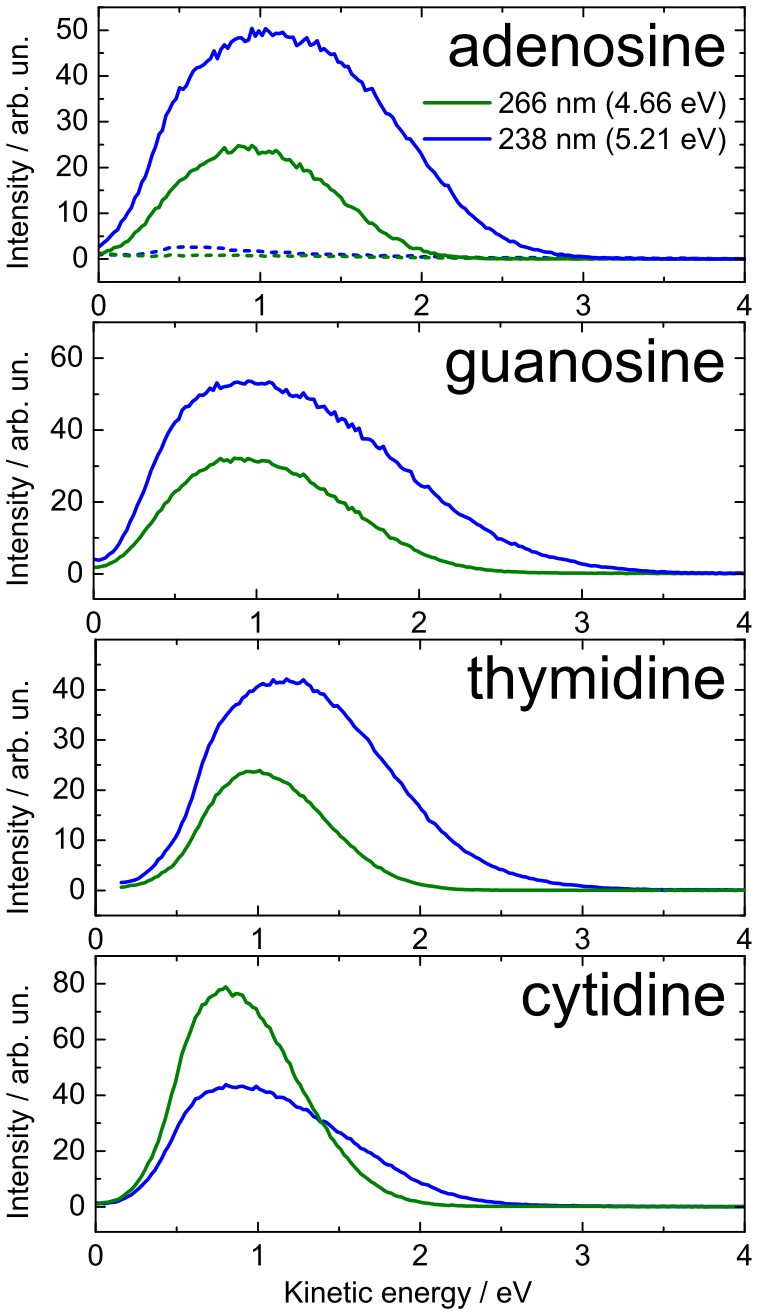

Figure S2: One-color two-photon photoelectron spectrum of aqueous nucleosides.

energies above 10 eV. Below 10 eV, the cross-sections for these two processes decrease by at least five orders of magnitude. In the present work, UV pulses are used and photoelectrons with kinetic energies below 3 eV are generated. Thus, ionization and electronic excitation are negligible. Dissociative electron attachment to water molecules is important at kinetic

energies around $6 - 10\,\mathrm{eV}$. Dissociative electron attachment to solute molecules, however, may be important at lower kinetic energies.[S5,S6] Nevertheless, this process decrases the total signal at a given kinetic energy but will not contribute signal at another energy. The remaining inelastic processes are excitation of vibrational and rotational states. Corresponding cross-sections are at least one order of magnitude smaller than the one for elastic scattering.

Another related issue is the electron range in liquid water and to what extend photoelectron kinetic energy at low kinetic energy is surface or bulk sensitive. In a previous work, we have conservatively estimated that for few eV electrons the probing depth is about $5\,\mathrm{nm}$,[S7] i. e. allowing for both, surface and bulk signal. Similar results are reported by Suzuki et al., who find effective attenuation lengths on the order of $2 - 3\,\mathrm{nm}$.[S8] These findings are in excellent agreement with earlier experimental work[S9] and theoretical investigations.[S4] The particular role of elastic processes to the very low effective attenuation length of photoelectrons in liquids was also discussed by Thürmer et al.[S10] These findings clearly show, that liquid-jet photoelectron spectroscopy at low kinetic energies contains both - signal from the surface and from the bulk.

S3 Time-dependent photoelectron spectra and global fitting

We have analyzed our experimental data taking into account different numbers of involved states / relaxation paths. Fig. S3 shows the analysis for thymine for considering two, three and four decays, respectively. The thymidine fit results considering two, three and four components are shown in Fig. S4. Considering only one component for each delay direction results in systematic residues in the fitting. Fit results are summarized in table S1.

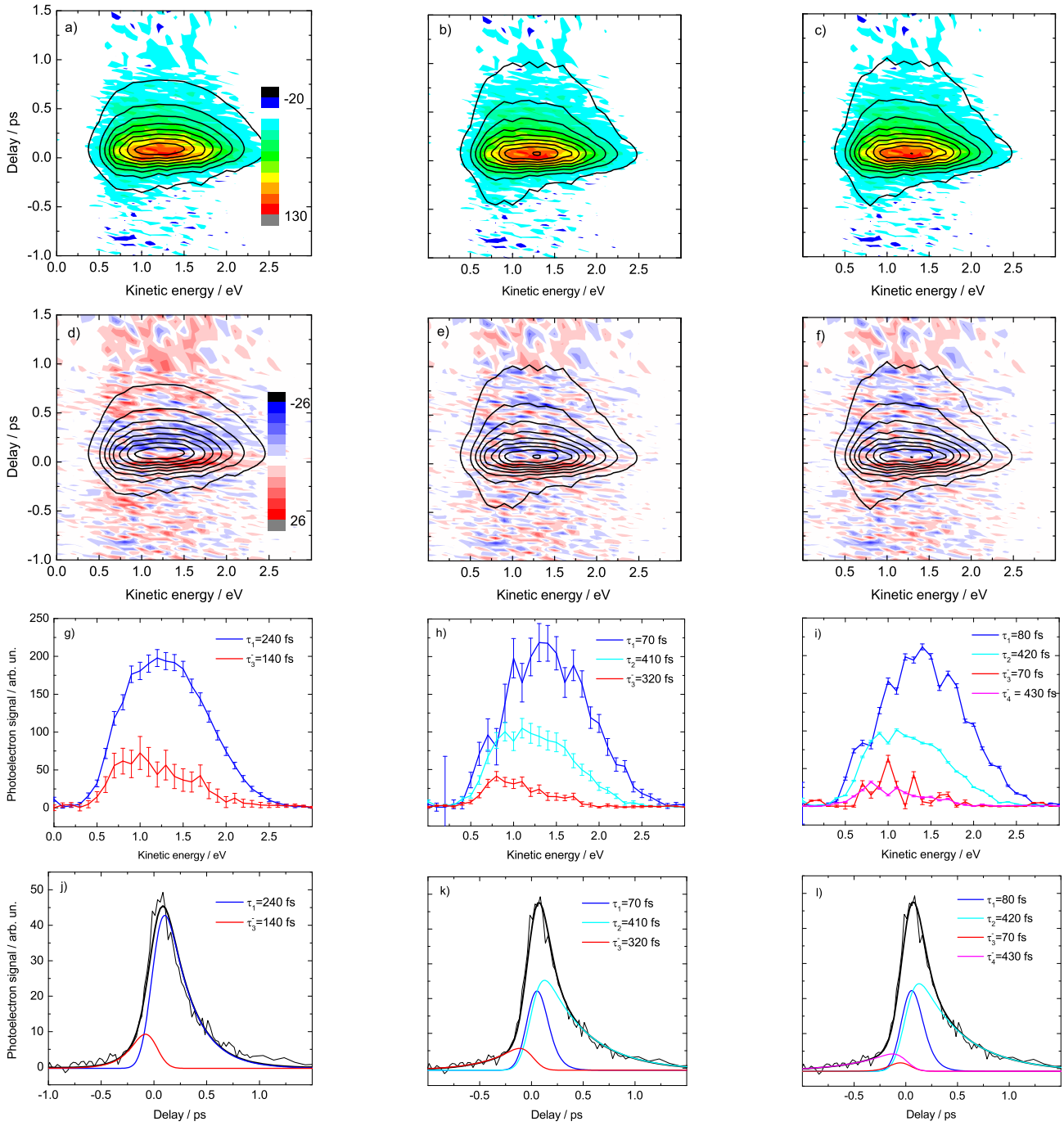

Figure S3: Time-resolved photoelectron spectrum of thymine, globally analyzed by two (a, d, g, j), three (b, e, h, k) or four (c, f, i, l) spectral contributions. a-c) Comparison between data (color) and global fit (contour lines), d-f) residuals (color) and global fit (contour lines), g-i) Decay associated spectra, j-l) Population dynamics of individual contributions. The color scale of the residuals covers a range of ±20% of the maximum photoelectron signal. In h) the maximum kinetic energies are indicated by vertical lines.

Table S1: Summary of fitparameters and comparison with fluorescence upconversion results.[S11,S12] τ_{1-4} are derived lifetimes, where the superscript $-$ refers to the value obtained for negative delay direction. $A_i = \int_0^\infty A_i(E_{\mathrm{kin}})\mathrm{d}E_{\mathrm{kin}}$ is the energy integrated signal associated with decay i at delay = 0. $\beta = \frac{A_3^- + A_4^-}{A_1^+ + A_2^+}$ is the ratio between signal in negative delay direction to signal in positive delay direction. Uncertainties given correspond to one standard deviation as obtained from the fit.

		τ_1 / fs	τ_2 / fs	τ_3^- / fs	τ_4^- / fs	β
Thy (266 nm / 238 nm)	2 comp.	240 ± 10	–	140 ± 40	–	0.29
	3 comp.	70 ± 10	410 ± 40	320 ± 40	–	0.08
	4 comp.	80 ± 10	420 ± 10	70 ± 10	430 ± 10	0.14
Thy (266 nm / 330 nm)	FU[S11]	195 ± 17	633 ± 18	–	–	–
Thd (266 nm / 238 nm)	2 comp.	260 ± 10	–	230 ± 30	–	0.13
	3 comp.	120 ± 10	390 ± 10	300 ± 20	–	0.09
	4 comp.	140 ± 10	430 ± 10	3 ± 10	310 ± 10	0.73
Thd (266 nm / 340 nm)	FU[S12]	150 ± 20	720 ± 30	–	–	–

S4 Longer timescan

In S5 we show the same data from S3 but displayed for a longer delay range together with the global analysis considering three components.

S5 Potential energy profiles for isolated thymine

Figure S6 shows the potential energy profiles between $(S_0)_{\mathrm{min}}$ and MECI at the CASPT2 level. This figure corresponds to Fig. 3a in Ref.[S13] The slight descrepancy in number is due to the slightly different level of theory. The potential energy difference between nπ^* and $\pi\pi^*$ state for in total 30 trajectories are shown in Figure S7. 24 trajectories are found to reach the $(\pi\pi^*(\mathrm{C5-C6})/\mathrm{S_0})_{\mathrm{CI}}$ regions, while 6 reach the $(\pi\pi^*(\mathrm{C4-O8})/\mathrm{S_0})_{\mathrm{CI}}$ regions.

S6 Discussion of bulk and surface contributions

The relatively high sensitivity of photoelectron spectroscopy at low kinetic energies to both, surface and bulk motivates an alternative assignment of the observed contributions to bulk and surface species. We will show that this leads to a contradiction and can therefore be

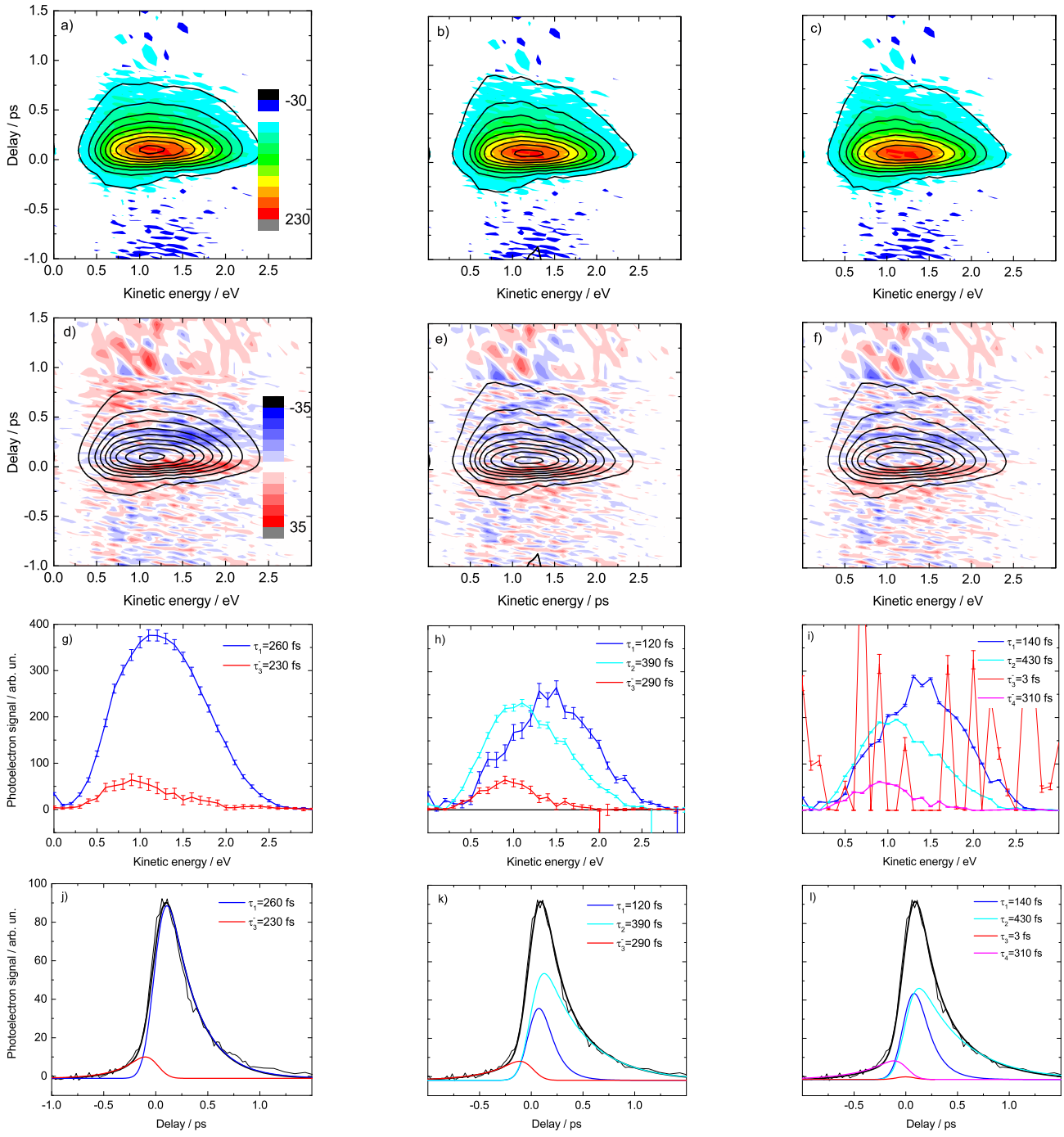

Figure S4: Time-resolved photoelectron spectrum of thymidine, globally analyzed by two (a, d, g, j), three (b, e, h, k) or four (c, f, i, l) spectral contributions. a-c) Comparison between data (color) and global fit (contour lines), d-f) residuals (color) and global fit (contour lines), g-i) Decay associated spectra, j-l) Population dynamics of individual contributions. The color scale of the residuals covers a range of ±15% of the maximum photoelectron signal. In h) the maximum kinetic energies are indicated by vertical lines.

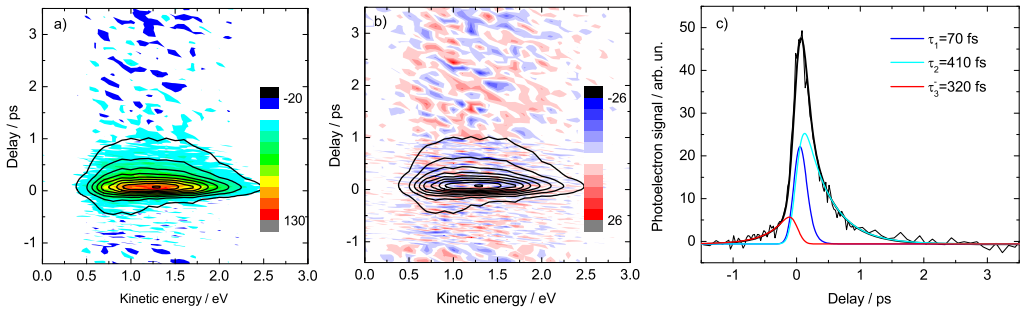

Figure S5: Time-resolved photoelectron spectrum of thymine for a longer time range (same dataset and color scales as in S3). Data are globally analyzed by three spectral components.

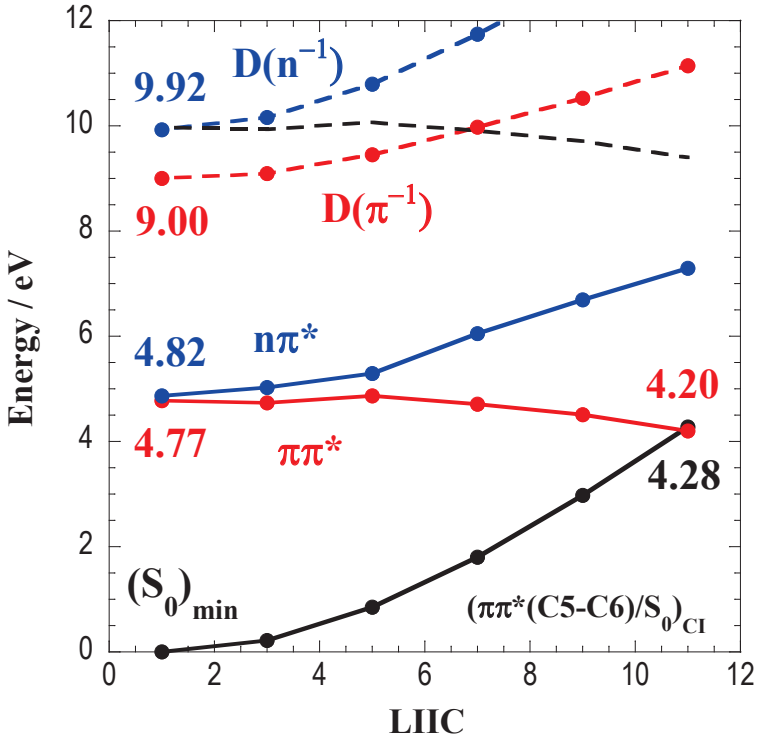

Figure S6: Potential energy profiles from $(S_0)_{min}$ to $(\pi\pi^*(C5-C6)/S_0)_{CI}$ using LIIC points at the CASPT2(12,9) and CASPT2(11,9) levels for the neutral and cationic molecules, respectively. The energies of the cationic states are shifted using the correction described in the text. The dashed line shows the energy $E(\pi\pi^*)+5.2\,\mathrm{eV}$ along the LIIC points. The energies of the $\pi\pi^*$, $n\pi^*$, $D(\pi^{-1})$, and $D(n^{-1})$ states at $(S_0)_{min}$ and MECI structures are also shown.

discarded.

As already discussed in detail in Sec. S2, the small effective attenuation length at these kinetic energies is almost entirely due to elastic effects. Inelastic processes can be neglected. Therefore, both the different photoelectron spectra and the different lifetimes would have to

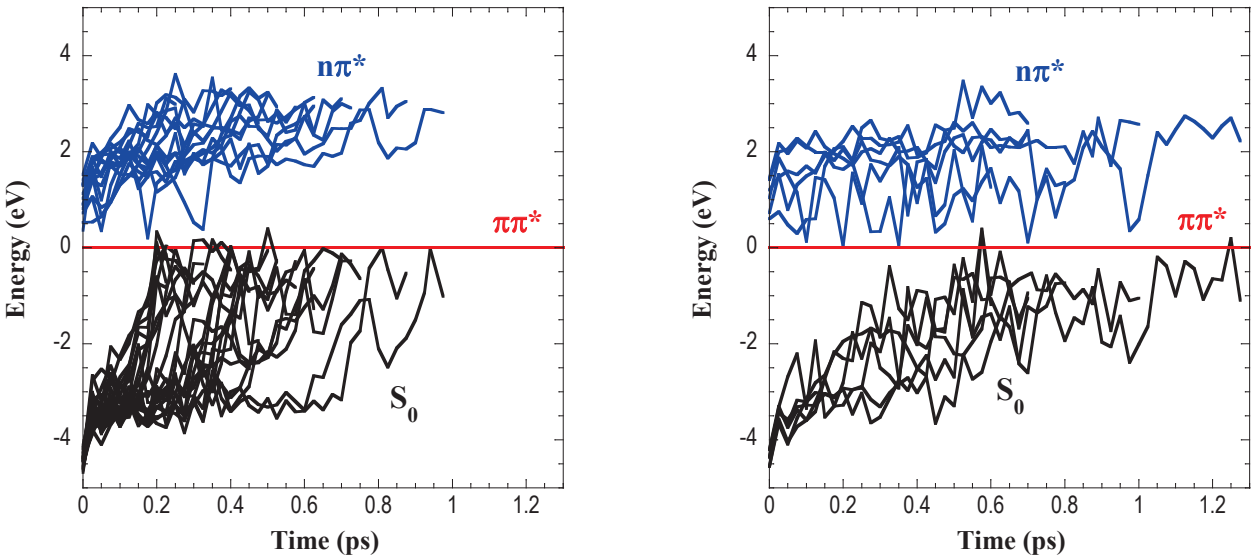

Figure S7: Potential energy differences between the nπ^* and $\pi\pi^*$ states, ($E(\mathrm{n}\pi^*) - E(\pi\pi^*)$; blue lines), and the S_0 and $\pi\pi^*$ states, ($E(S_0) - E(\pi\pi^*)$; black lines) along the trajectories that reach the $(\pi\pi^*(\mathrm{C5-C6})/S_0)_{\mathrm{CI}}$ (left) and $(\pi\pi^*(\mathrm{C4-O8})/S_0)_{\mathrm{CI}}$ (right) regions.

be attributed to the different environments of the molecules. The different spectra are not due to different paths of the photoelectrons.

The situation at the water surface is difficult to be predicted: the exact solvation structure is not known and it was shown that depending on where hydrogen bonds are formed, the effect on the ionization energy is very different.[S14] However, we can derive important conclusions from the comparison of the data for Thy and Thd. Due to the presence of the polar ribose moiety in Thd, Thd is expected to be less surface-active than Thy. I. e. the contribution that is more important in Thd than in Thy would be assigned to originate from the bulk. This is the slower decaying contribution at lower kinetic energies, i. e. larger binding energies. Hence, the contribution at larger kinetic energies (lower binding energies) would be assigned to the surface.

On the other hand, it is reasonable to assume that the electron binding energies in molecules at the surface are in between those of the gas phase and the bulk values. This is also supported by studies by Ghosh et al.,[S14] who investigated the effect of microsolvation and of different number of solvation shells on the vertical ionization energy. I. e. we would

expect, that the surface contribution is stronger bound than the bulk contribution (cf. Fig. 1 of the manuscript). This is in contradiction to the before-mentioned argumentation on the surface affinity of the molecules.

Further arguments against an assignment to surface and bulk contributions come from our previous work on adenine and adenosine.[S15] Although adenine is a purine base while Thy is a pyrimidine base we expect similar behavior in terms of surface affinity. In case of adenosine we have observed a single contribution, in case of adenine we saw contributions from the two different tautomers present in solution, but in no case we found any indication for two different signals arising from bulk and surface. In case of adenosine we have also investigated the concentration dependence and found a linear relation between signal and concentration.

Therefore, we argue that the two different signals observed for thymine and thymidine cannot be assigned to bulk and surface.

References

[S1] Jarvis, G. K.; Evans, M.; Ng, C. Y.; Mitsuke, K. *J. Chem. Phys.* **1999**, *111*, 3058.

[S2] Preissler, N.; Buchner, F.; Schultz, T.; Lübcke, A. *J. Phys. Chem. B* **2013**, *117*, 2422.

[S3] Winter, B.; Faubel, M. *Chem. Rev.* **2006**, *106*, 1176.

[S4] Plante, I.; Cucinotta, F. A. *New J. Phys.* **2009**, *11*, 063047.

[S5] Bao, X.; Wang, J.; Gu, J.; Leszczynski, J. *Proc. Nat. Acad. Sci.* **2006**, *103*, 5658.

[S6] Smyth, M.; Kohanoff, J. *Phys. Rev. Lett.* **2011**, *106*, 238108.

[S7] Buchner, F.; Schultz, T.; Lübcke, A. *Phys. Chem. Chem. Phys.* **2012**, *14*, 5837.

[S8] Suzuki, Y.-I.; Nishizawa, K.; Kurahashi, N.; Suzuki, T. *Phys. Rev. E* **2014**, *90*, 010302(R).

[S9] Konovalov, V. V.; Raitsimring, A. M.; Tsvetkov, Y. D. *Int. J. Rad. Appl. Instr. C Rad. Phys. Chem.* **1988**, *32*, 623.

[S10] Thürmer, S.; Seidel, R.; Faubel, M.; Eberhardt, W.; Hemminger, J. C.; Bradforth, S. E.; Winter, B. *Phys. Rev. Lett.* **2013**, *111*, 173005.

[S11] Gustavsson, T.; Bányász, A.; Lazzarotto, E.; Markovitsi, D.; Scalmani, G.; Frisch, M. J.; Barone, V.; Improta, R. *J. Am. Chem. Soc.* **2006**, *128*, 607.

[S12] Onidas, D.; Markovitsi, D.; Marguet, S.; Sharonov, A.; Gustavsson, T. *J. Phys. Chem.B* **2002**, *106*, 11367.

[S13] Nakayama, A.; Arai, G.; Yamazaki, S.; Taketsugu, T. *J. Chem. Phys.* **2013**, *139*, 214304.

[S14] Ghosh, D.; Isayev, O.; Slipchenko, L. V.; Krylov, A. I. *J. Phys. Chem. A* **2011**, *115*, 6028.

[S15] Buchner, F.; Ritze, H.-H.; Lahl, J.; Lübcke, A. *Phys. Chem. Chem. Phys.* **2013**, *15*, 11402.